Journal of Translational Medicine

RESEARCH

Open Access

C/D box small nucleolar RNA SNORD104 promotes endometrial cancer by regulating the 2′-O-methylation of *PARP1*

Bingfeng Lu, Xi Chen, Xin Liu, Jingwen Chen, Honglei Qin, Shuo Chen and Yang Zhao*

Abstract

Background: Small nucleolar RNAs (snoRNAs) are dysregulated in many cancers, although their exact role in tumor genesis and progression remains unclear.

Methods: The expression profiles of snoRNAs in endometrial cancer (EC) tissues were analyzed using data from The Cancer Genome Atlas, and SNORD104 was identified as an upregulated snoRNA in EC. The tumorigenic role of SNORD104 in EC was established in CCK8, colony formation, EdU, apoptosis, Transwell, and in vivo xenograft experiments. The molecular mechanisms of SNORD104 were analyzed by RNA immunoprecipitation (RIP), Nm-seq, RTL-P assay, RNA stability assay, qRT-PCR, and western blotting.

Results: Antisense oligonucleotide (ASO)-mediated knockdown of SNORD104 in Ishikawa cells significantly inhibited their proliferation, colony formation ability, migration, and invasion in vitro and increased apoptosis. On the other hand, overexpression of SNORD104 promoted EC growth in vivo and in vitro. RIP assay showed that SNORD104 binds to the 2′-O-methyltransferase fibrillarin (FBL), and according to the results of Nm-seq and RTL-P assay, SNORD104 upregulated *PARP1* (encoding poly (ADP-ribose) polymerase 1) 2′-O-methylation. The binding of FBL to *PARP1* mRNA was also verified by RIP assay. Furthermore, SNORD104 expression was positively correlated with *PARP1* expression in EC tissues. In the presence of actinomycin D, SNORD104 increased the stability of *PARP1* mRNA and promoted its nuclear localization. Finally, silencing *FBL* or *PARP1* in the HEC1B cells overexpressing SNORD104 inhibited their proliferative and clonal capacities and increased apoptosis rates.

Conclusions: SNORD104 enhances *PARP1* mRNA stability and translation in the EC cells by upregulating 2′-O-methylation and promotes tumor growth.

Keywords: SNORD104, 2′-O-methylation, Fibrillarin, *PARP1*, Endometrial cancer

Introduction

Endometrial cancer (EC) is one of the most common malignancies in menopausal and postmenopausal women in developed countries, and its incidence is increasing worldwide [1, 2]. Although surgery, chemotherapy, and radiotherapy have achieved satisfactory outcomes, the survival rate of EC patients is still dismal due to the tendency of the tumor cells to relapse and metastasize [3]. Therefore, it is crucial to elucidate the molecular mechanisms underlying the initiation, progression, and metastasis of EC in order to identify potential therapeutic targets for personalized treatment. Small nucleolar RNAs (snoRNAs) are a class of small non-coding RNAs (ncRNAs) with conserved structural elements that are widely distributed in the nucleolus of eukaryotic cells and

*Correspondence: yida.zhaoyang@163.com

Department of Obstetrics and Gynecology, Department of Gynecologic Oncology Research Office, Guangdong Provincial Key Laboratory for Major Obstetric Diseases, The Third Affiliated Hospital of Guangzhou Medical University, No. 63 Duobao Raod, Liwan District, Guangzhou 510150, Guangdong, People's Republic of China

broadly classified into the C/D box snoRNAs (SNORDs) and H/ACA box snoRNAs [4]. They are usually encoded by intron regions of coding genes or non-coding genes and are complicated by the transcription and processing of host genes, with only a few being encoded by independent genomic locations [5]. The snoRNAs were long considered to be involved in the nucleolar function. Recent studies show that snoRNAs mediate 2′-O-methylation and pseudouridylation of rRNA, tRNA, mRNA, snRNA, and other RNAs via complementary base pairing and also regulate gene expression by forming snoRNP complexes with ribonucleolar proteins (RNPs) [6, 7]. We identified the snoRNAs potentially related to the development of EC by screening the transcriptomic data of The Cancer Genome Atlas (TCGA) database. SNORD104 (located at 17q23.3, also known as U104) was significantly upregulated in the EC tissues, although its role in cancer, particularly EC, remains unclear.

Fibrillarin (FBL) is a component of the small nucleolar ribonucleoprotein (snRNP) (including FBL, NOP56, NOP58) that contains N-terminal repeat domains rich in glycine and arginine residues, similar to the FBLs in other species. The central region of FBL resembles an RNA binding domain and contains a common RNP sequence [8]. FBL is a key 2′-O-ribose methylase that catalyzes SNORD-dependent methylation of target RNAs [9]. However, whether FBL-catalyzed 2′-O-methylation plays an important role in EC remains unknown. In this study, we evaluated the oncogenic effects of SNORD104 in EC through established in vitro and in vivo experiments, and explored the molecular mechanisms by 2′-O-methylation sequencing (Nm-seq) and RNA immunoprecipitation.

Methods

Human tissue samples

Tumor tissue samples were collected from 71 treatment-naïve EC patients who underwent surgery at the Third Affiliated Hospital of Guangzhou Medical University. The samples were snap frozen in liquid nitrogen immediately after resection and stored at − 80 °C. The study protocol was approved by the ethics committee of the hospital, and all patients provided written informed consent.

Cell culture and transfection

Human EC cell lines (Ishikawa, HEC1A, HEC1B, and KLE) and immortalized endometrial cells (EEC) were purchased from ATCC (Manassas, VA, USA) or Jennio Biotech (Guangzhou, China). HEC1B cells were cultured in DMEM (HyClone, Logan, UT, USA), HEC1A and Ishikawa cells in RPMI-1640 medium (HyClone), and the KLE cells in DMEM-F12 (HyClone). All media were supplemented with 10% fetal bovine serum (FBS; Gibco, Grand Island, NY, USA) and 100 U/ml penicillin and streptomycin (Gibco). The cell lines were incubated at 37 °C under 5% CO_2. As per the experimental requirements, the cells were transfected with SNORD104 ASO (TCTTTCTCGTAAATGCTGAG), si-*FBL* (GGGCTA AGGTTCTCTACCT), or si-*PARP1* (CACGGACTC TCTACCGTAT) using Lipofectamine 3000 (Invitrogen, Carlsbad, CA, USA) according to the manufacturer's instructions. The oligonucleotides were synthesized by RIBOBIO (Guangzhou, China).

Bioinformatics analysis

The clinical and transcriptomic data of EC were downloaded from https://portal.gdc.cancer.gov/projects/TCGA-UCEC, ITPR3, LMNB1, PARP1, PARP4, and TUBA1C protein expression in EC tissues was analyzed using the CPTAC [10] database (http://ualcan.path.uab.edu). The correlation between PARP1 expression and prognosis of EC patients was evaluated by Kaplan–Meier survival analysis using KMplot [11] (http://kmplot.com).

Cell viability assays

The cells were seeded in a 96-well plate at the density of 2000 cells/100 µl per well and transfected with the respective constructs. The CCK8 reagent (Yeasen Biotechnology, Shanghai, China) was added to the cells at 0, 24, 48, and 72 h, and the absorbance of each well was measured at 450 nm using a microplate reader (BioTek, Winooski, VT, USA). The experiment was repeated thrice.

Colony formation assay

The cells were seeded in a 6-well plate at the density of 500 cells/2 ml per well and transfected with the respective constructs once they adhered. After culturing for 7–10 days, the colonies were fixed using formaldehyde for 15 min, washed thrice with PBS, and stained with crystal violet for 10 min. The plates were rinsed with tap water to remove the excess dye and dried, and the number of colonies was counted.

EdU assay

The Ishikawa/HEC1B cells were seeded in 96-well plates, and EdU solution (Thermo Scientific, USA) was added. The cells were incubated for 16 h, and the subsequent steps were followed as per the manufacturer's instructions. The stained cells were observed under a microscope (Olympus, Tokyo, Japan).

Apoptosis assay

Apoptosis was detected by propidium iodide (PI) and fluorescein isothiocyanate (FITC)-Annexin V (BD Pharmingen, San Diego, CA, USA) staining according to the manufacturer's instructions. Briefly, the cells

were harvested 48 h after transfection and washed twice with cold PBS. The suspension was stained with 100 µl 1 × buffer and 5 µl FITC-Annexin V and PI in the dark for 15 min. The reaction was terminated by adding 400 µl 1 × buffer, and the cells were analyzed by flow cytometry within 1 h.

Quantitative real-time reverse transcription PCR

Total RNA was extracted from EC cell lines or tissues using TRIzol reagent (1 ml; Takara, Shiga, Japan) and reverse transcribed to cDNA. Quantitative real-time PCR was performed using the SYBR PreMix Ex TAQ II kit (Takara). The primer sequences were as follows: U6: forward: 5′ CTCGCTTCGGCAGCACA 3′; reverse: 5′ AACGCTTCACGAATTTGCGT 3′; *GAPDH*: forward: 5′ CCCATCACCATCTTCCAGGAG 3′; reverse: 5′ GTT GTCATGGATGACCTTGGC 3′; SNORD104: forward: 5′ CATTCCAATTAAAGCACG 3′; reverse: 5′ CAGACT CCAGTTCGCATC 3′; *PARP1*: forward: 5′ CGGAAC AAGGATGAAGTGAA 3′; reverse: 5′ TTGGTGGAG GCGGAGA 3′; *PARP4*: forward: 5′ TAGCCTGGTCAT TTGGT 3′; reverse: 5′ AGATGGCATTCTTCACG 3′; 18S: forward: 5′ GAAACGGCTACCACATCC 3′; reverse: 5′ ACCAGACTTGCCCTCCA 3′; *ITPR3*: forward: 5′ CCAAGCAGACTAAGCAGGACA 3′; reverse: 5′ ACA CTGCCATACTTCACGACA 3′; *LMNB1*: forward: 5′ AAGCATGAAACGCGCTTGG 3′; reverse: 5′ AGTTTG GCATGGTAAGTCTGC 3′; *TUBA1C*: forward: 5′ TGT TTGTAGACTTGGAACCCAC 3′; reverse: 5′ GCCAAT GGTGTAGTGCCCT 3′.

Western blotting

Total protein was extracted from cultured cells or tissues using radioimmunoprecipitation assay (RIPA) buffer containing protease inhibitors and quantified using the BCA Protein Assay Kit (Beyotime, China). The protein samples were diluted with the appropriate amount of loading buffer and PBS to 2 µg/l, and denatured by heating at 95 °C for 15 min. The samples were resolved by 10% or 12% sodium dodecyl sulfate polyacrylamide gel electrophoresis (SDS-PAGE) and transferred to polyvinylidene fluoride (PVDF) membranes (Amersham, Munich, Germany). Following overnight incubation with rabbit anti-FBL (1:2000 Magna, Proteintech, Rosemont, IL, USA), rabbit anti-PARP1 (1:2000 Magneto, Proteintech), rabbit anti-PARP4 (1:2000, Bioss, Woburn, MA, USA), anti-ITPR3 (1:2000, LSBio), anti-LMNB1 (1:10,000, Proteintech), anti-Vinculin (1:10,000, Proteintech), anti-GAPDH (1:5000, Proteintech) and anti-α-tubulin (TUBA1B/1C) (1:2000, Proteintech) antibodies at 4 ℃, the membranes were washed thrice with 1% Tris-buffered saline-Tween20 (TBST) buffer for 10 min each time. The membranes were then incubated with the secondary antibody for 2 h, and washed again with 1% TBST buffer for 10 min. The bands were visualized using an enhanced chemiluminescence system (NCM Biotech, Suzhou, China), and the protein levels were quantified using grayscale values.

RNA immunoprecipitation (RIP) assay

RIP assay was performed using the Magna RIP RNA-Binding Protein Immunoprecipitation Kit (Millipore, Bedford, MA, USA) as per the manufacturer's instructions. Cells growing at 80–90% confluence were harvested and lysed using RIPA lysis buffer. The cell extracts were incubated with magnetic beads with anti-mouse FBL (Santa Cruz Biotechnology, Santa Cruz, CA, USA) or normal mouse IgG (negative control) in the RIPA lysis buffer. After digesting the protein using protease K, the immunoprecipitated RNA was isolated and analyzed using qRT-PCR.

Nm-seq analysis

Nm-sequencing was performed by the Shanghai Cloud-seq Biotech Co. Ltd. as previously described [12] using the Illumina NovaSeq 6000 sequencer.

Reverse transcription at low dNTPs-PCR (RTL-P) assay

RTL-P assay was performed to detect the 2′-O-methylation level (Nm) of PARP1 according to published methods [13, 14]. Briefly, 5 µg total RNA was incubated with low (1 µM) or high (1 mM) concentration of dNTPs (Takara) and 1 µl specific RT primers at 65 °C for 5 min and then placed on ice. The reaction was performed using 4 µl M-MLV RT 5 × buffer (PROMEGA), 1 µl 200 U/µl M-MLV Reverse Transcriptase (PROMEGA), 1 µl 0.1 M DTT (PROMEGA), and 1 µl 40 U/µl RNase inhibitor (PROMEGA) at 50 °C for 1 h, and then at 70 °C for 15 min. QRT-PCR was performed on the SYBR Prime X Ex-TAQ Patent II Suite (Takara) using PARP1-specific primers. The relative expression of the gene was calculated by comparing the period threshold (Ct) of the target gene in the experimental group and the control group at low concentrations according to the $2^{-\Delta Ct}$ method.

RNA stability assay

Stably transfected cells were seeded into a 6-well plate and incubated until they reached 70% confluence. Actinomycin D (Sigma, St. Louis, MO, USA) was added (Act D, 5 µg/ml), and the cells were harvested at 0, 6, and 12 h. Total RNA was extracted using TRIzol reagent, and *PARP1* mRNA levels were detected by qRT-PCR.

Nucleocytoplasmic separation assay

The confluent cells were harvested using a scraper and centrifuged at 1500 rpm for 5 min. The supernatant was removed, and the nuclear and cytoplasmic fractions were

extracted from the cells using a specific kit (Beyotime, Shanghai, China). Both fractions were analyzed by western blotting as per standard protocols.

Nude mouse xenograft assay

All animal experiments were conducted in accordance with the guidelines of the National Institute of Health on the Care and Use of Experimental Animals and were approved by the Animal Care and Use Committee of Guangzhou Medical University. Four-week-old female BALB/c nude mice were purchased from Guangdong Experimental Animal Center (Foshan, China) and housed under controlled temperature and light (12 h dark/12 h light) with ad libitum access to food and water. The mice were injected subcutaneously into their right flanks with 1×10^7 tumor cells suspended in 200 µl of FBS-supplemented culture medium. The tumors were measured twice a week, and the volume was calculated according to the formula (length × width^2)/2. At the end of the experiment (or when the mice died), the mice were euthanized, and the tumors were excised.

Statistical analysis

GraphPad Prism [version 8.02(263)] was used for statistical analysis. Non-parametric Mann–Whitney test for small samples that do not meet the normal distribution; Student's t-test was used for the normal distribution and when the sample size was large; Correlations between groups were determined using the Pearson correlation coefficient. The CCK-8 assay data were analyzed using ANOVA. All data were presented as the mean ± S.D of at least three independent experiments. Statistical significance was set at $P < 0.05$.

Results

SNORD104 is upregulated in EC tissues

We analyzed the transcriptomic profiles of 548 EC tissue samples and 35 normal endometrial tissue samples from TCGA datasets (Fig. 1A), and found that SNORD104 was upregulated in the EC samples. To verify these results, we analyzed the expression of SNORD104 in post-operative EC tissues collected from the Third Affiliated Hospital of Guangzhou Medical University and analyzed the correlation between the expression of SNORD104 and clinicopathological features (Additional file 1: Table S1). SNORD104 expression was higher in patients with stage III/IV disease (n = 13) compared to those with stage I/II disease (n = 46) (Fig. 1B). In addition, SNORD104 was upregulated in the poorly differentiated (n = 15) versus the moderately or well-differentiated (n = 44) tumors (Fig. 1C). SNORD104 expression was also higher in patients with deep myometrial invasion (n = 26) compared to those with shallow myometrial invasion (n = 33) (Fig. 1D), as well as in patients with lymph node metastasis (n = 26) relative to those without lymph node metastasis (n = 33) (Fig. 1E). In contrast, there was no significant correlation between SNORD104 expression and vascular invasion (Fig. 1F). Therefore, we hypothesized that SNORD104 functions as an oncogene in EC.

SNORD104 knockdown inhibited the malignant potential of EC cells in vitro

Genome sequence analysis showed that SNORD104 was processed from the first intron region of the primary transcript of the *SNHG25* gene (small nucleolar RNA host gene 25, located at 17q21.3) (Fig. 1G), and the mature *SNHG25* RNA was transcribed from the exons. We found that *SNHG25* was also upregulated in EC tissues (Additional file 2: Fig. S1A, $^*P < 0.05$). In addition, SNORD104 was upregulated in the EC cell lines compared to that in the immortalized endometrial cells. Both SNORD104 and *SNHG25* were highly expressed in the Ishikawa cells, but showed relatively low expression levels in the HEC1B and HEC1A cells (Fig. 2A, Additional file 2: Fig. S1B, $^*P < 0.05$). Previous studies have shown that the host genes of snoRNAs regulate their respective snoRNAs and play a role in tumor development [15, 16]. To determine the role of SNORD104 and *SNHG25* in EC cells, we respectively transfected the Ishikawa cells with *SNHG25*-specific small interfering RNA (siRNA) and the HEC1B cells with SNHG25-overexpression plasmid, and an antisense oligonucleotide sequence (ASO) targeting SNORD104 in HEC1B cells. The knockdown efficiency was verified by qRT-PCR (Fig. 2B, Additional file 2: Fig. S1C, D, $^*P < 0.05$). SNORD104 knockdown significantly decreased the viability, proliferation (Fig. 2C, D, $^*P < 0.05$), clonal capacity (Fig. 2E, $P < 0.05$), migration, and invasion (Fig. 2G, $^*P < 0.05$) of Ishikawa cells, and increased the apoptosis rates (Fig. 2F, $^*P < 0.05$). In contrast, knocking down or overexpressing *SNHG25* had almost no effect on the proliferation and apoptosis of endometrial cancer cells (Additional file 2: Fig. S1E–H, ns means $P > 0.05$).

SNORD104 promotes EC progression in vitro *and* in vivo

HEC1B cells stably transfected with the SNORD104 plasmid (Fig. 3A, $^*P < 0.05$) exhibited high proliferative capacity (Fig. 3B–D, $^*P < 0.05$), along with increased invasion and migration rates (Fig. 3E, $^*P < 0.05$). Furthermore, SNORD104 overexpression reduced apoptosis rates of HEC1B cells (Fig. 3F, $^*P < 0.05$). Consistent with the in vitro results, HEC1B cells stably expressing SNORD104 formed significantly larger tumors in nude mice compared to the control cells inoculated with the empty vector (Fig. 3G, $^*P < 0.05$). Taken together, overexpression of SNORD104 significantly enhanced the

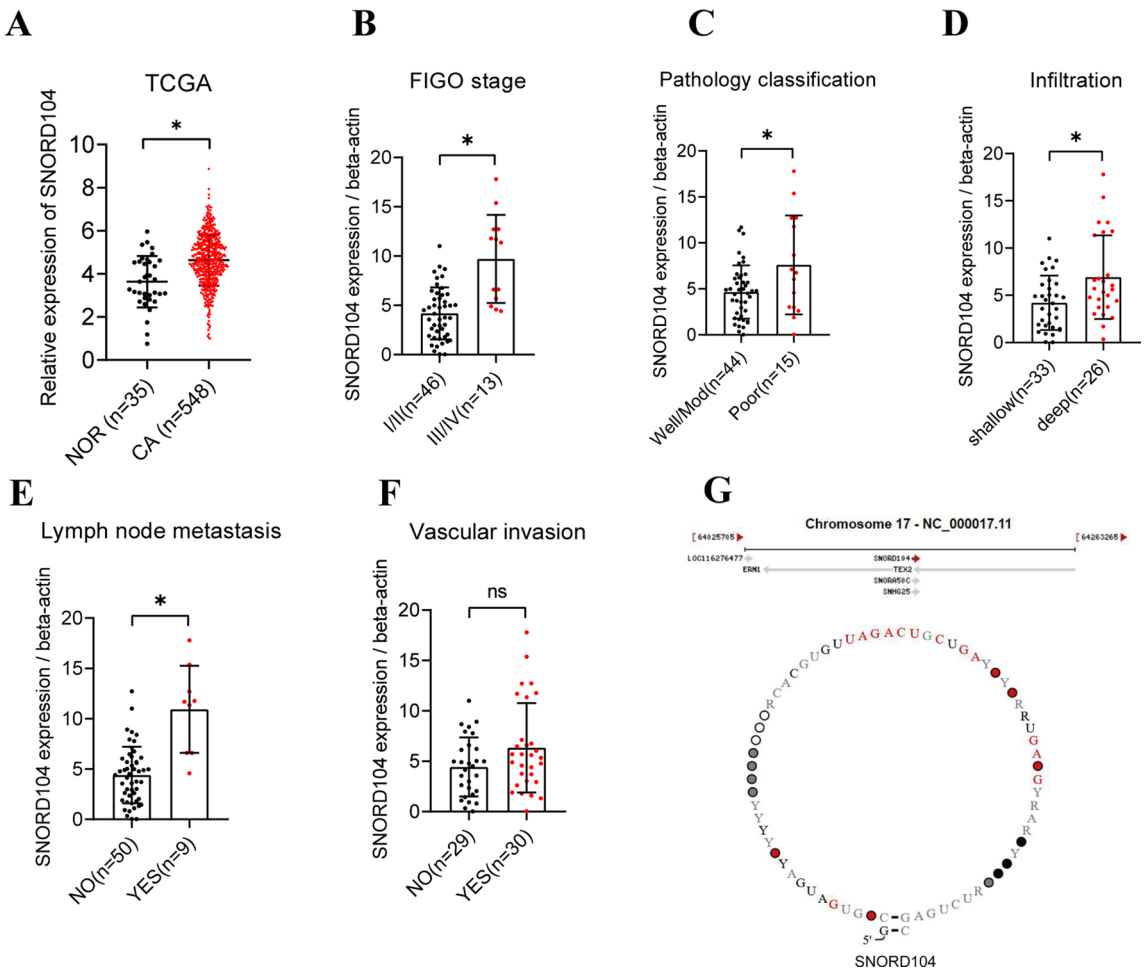

Fig. 1 SNORD104 is upregulated in EC tissues and associated with clinicopathological features. **A** TCGA data set analysis showing SNORD104 expression levels in EC tissue samples (n = 548) and normal endometrial tissue samples (n = 35). **B**–**F** Correlation of SNORD104 with FIGO stage, differentiation, myometrial invasion, lymph node metastasis, and vascular invasion. **G** Schematic and genomic location of SNORD104. Data were calculated and shown as the mean ± SD (error bars) from three independent experiments. *P < 0.05, ns means P > 0.05

proliferation, invasion, and migration of EC cells in vitro and promoted tumor growth in vivo.

SNORD0104 upregulates and stabilizes PARP1 by promoting 2′-O-methylation

The SNORDs and H/ACA box snoRNAs regulate gene expression via 2′-O-methylation and pseudouridylation, respectively. Therefore, we hypothesized that SNORD104 might be involved in FBL-mediated 2′-O-methylation. Indeed, the RIP assay of the lysates from SNORD104-overexpressing HEC1B cells using anti-FBL antibodies revealed significant enrichment of SNORD104 in the immuno-precipitate (Fig. 4A, *P < 0.05). However, SNORD104 overexpression did not affect the FBL protein level (Fig. 4B).

To identify potential target genes regulated by SNORD104-mediated 2′-O-methylation, we performed NM-seq in the control and SNORD104-overexpressing cells. As shown in Fig. 4C, 2′-O-methylation was upregulated (fold change ≥ 2) at 928 methylated sites (671 RNAs). It's reported small nucleolar RNAs generally guide the modification of target RNAs through complementary base pairing. Therefore, we intersect the RNAs with up-regulated 2′-O-methylation levels and the RNAs with complementary base pairing fragments of SNORD104. Next, we performed Kyoto Encyclopedia of Genes and Genomes (KEGG) pathway enrichment analysis of these hypermethylated RNAs. And the results showed that the apoptosis-related pathway ranked first (Fig. 4C). Further, we analyzed the enriched RNAs in apoptosis pathways, and the CPTAC database

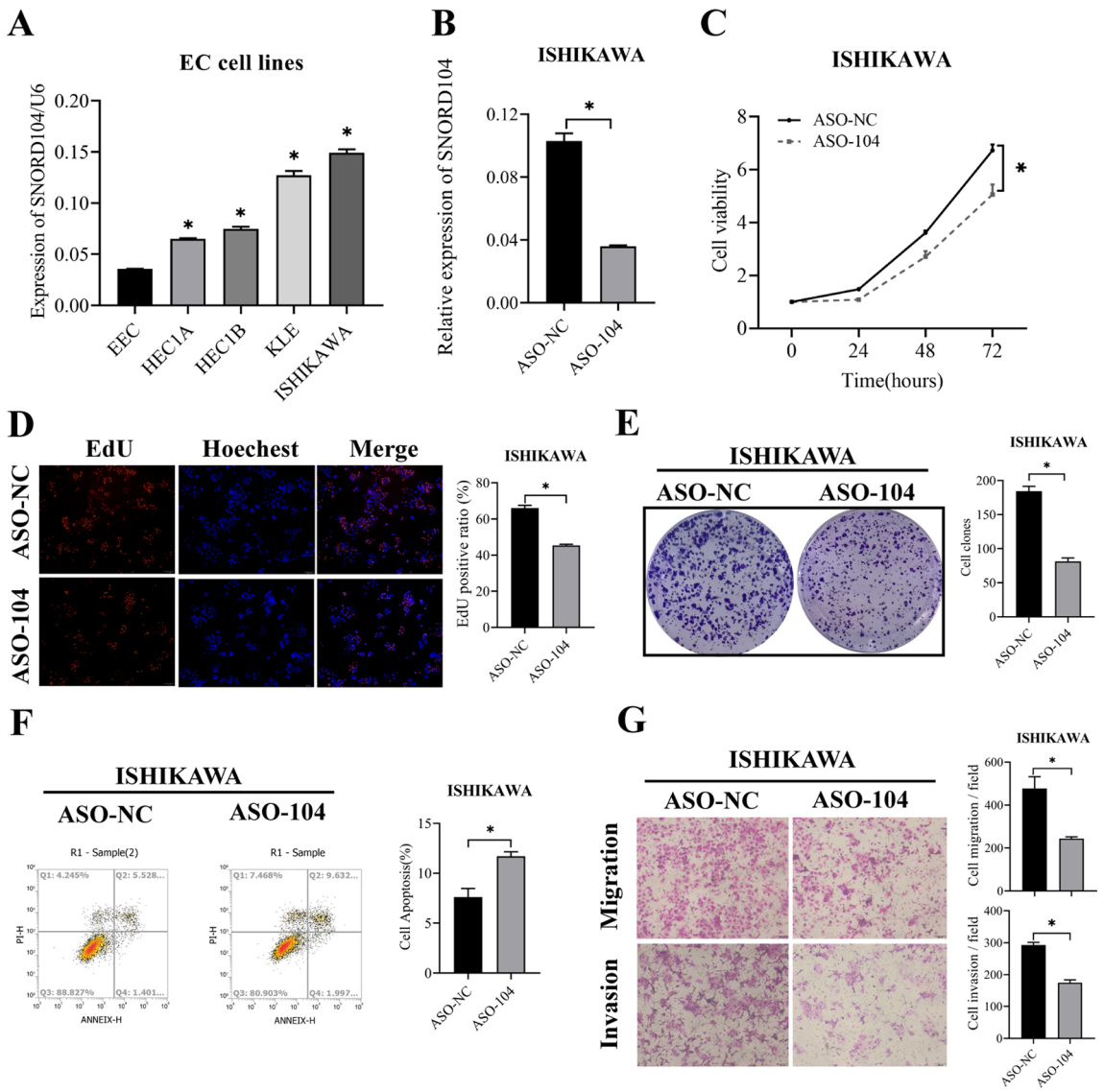

Fig. 2 SNORD104 knockdown repressed EC growth in vitro. **A** SNORD104 expression levels in EC cell lines and immortalized endometrial EEC cells. **B** Transfection of ASO in Ishikawa cells inhibited SNORD104 levels. **C** Viability, **D** Proliferation rates, **E** Colony formation, **F** apoptosis rates, and **G** migration and invasion of EC cells with SNORD104 knockdown. Data were calculated and shown as the mean ± SD (error bars) from three independent experiments. *P < 0.05

showed that their encoded proteins were upregulated in endometrial cancer tissues, including ITPR3, LMNB1, PARP1, PARP4, and TUBA1C (Additional file 3: Fig. S2A). Next, we used RIP assay to detect whether FBL protein binds to these 5 RNAs, and western blot to detect whether the proteins encoded by these 5 RNAs changed. The results show that only PARP1 mRNA binds to FBL protein (Fig. 4D, *P < 0.05), and only PARP1 mRNA and protein level changes (Fig. 4E, F, *P < 0.05). Therefore, we next analyzed the expression of *PARP1* in post-operative EC tissues and observed a positive correlation between SNORD104 and *PARP1* expression levels (Fig. 4G, *P < 0.05). PARP1 is primarily localized in the nucleus and is involved in DNA damage repair and ribosome biogenesis. Consistent with this, SNORD104 overexpression increased PARP1 protein levels in the nuclear fraction (Fig. 4H). In addition, the SNORD104-overexpressing xenografts also showed increased PARP1 protein levels (Fig. 4I, J).

RTL-P assay was next performed to detect the level of 2′-O-methylation in *PARP1* mRNA (Fig. 5A). SNORD104 knockdown and overexpression respectively decreased

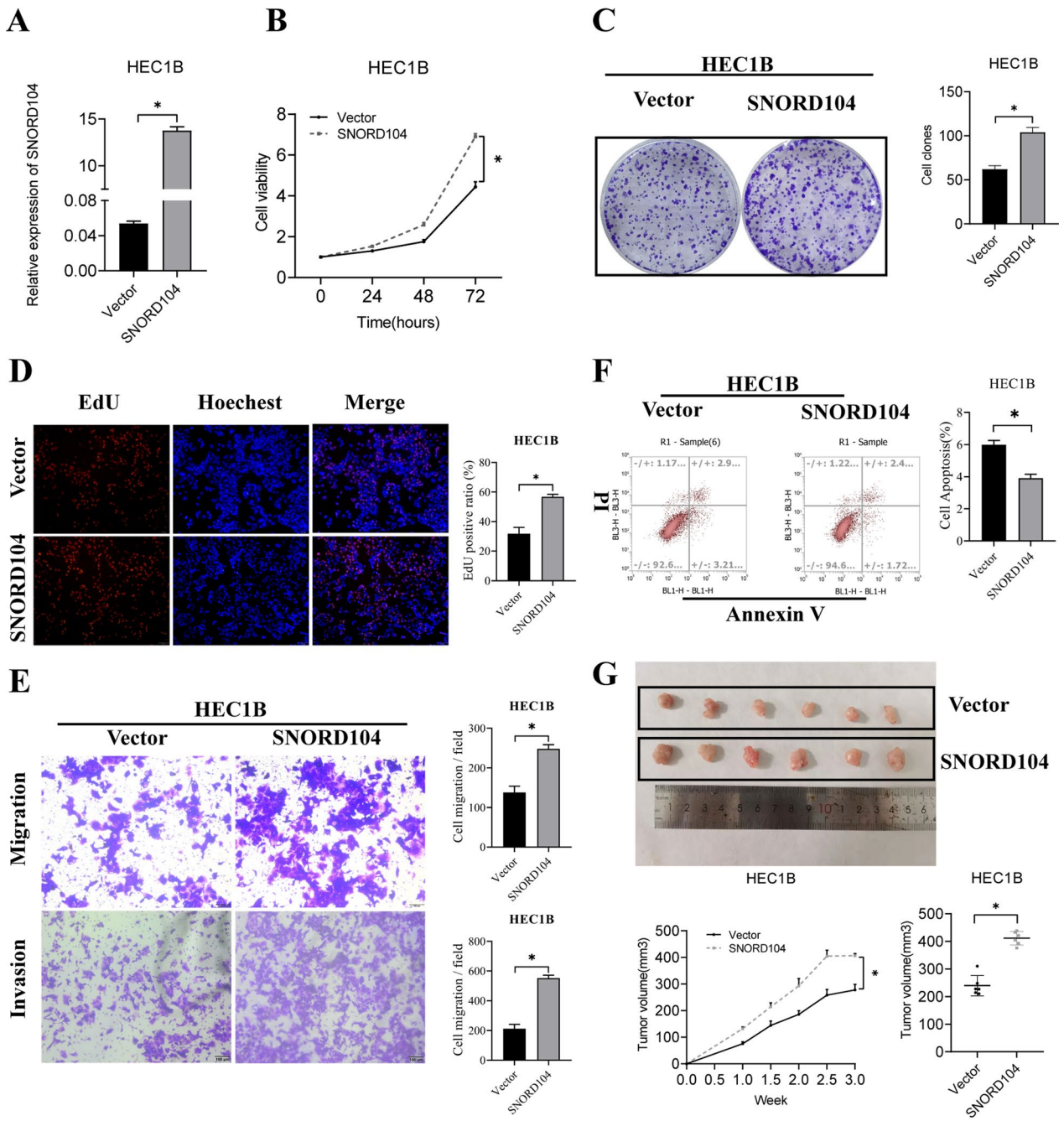

Fig. 3 SNORD104 overexpression promoted EC growth in vitro and in vivo. **A** SNORD104 expression in HEC1B cells transfected with the overexpression plasmid. **B** Viability, **C** colony formation, **D** proliferation rates, **E** apoptosis rates, and **F** migration and invasion of HECB1 cells overexpressing SNORD104. **G** Tumor volumes in nude mice inoculated with control or SNORD104-overexpressing HEC1B cells. Data were calculated and shown as the mean ± SD (error bars) from three independent experiments. *P < 0.05

and increased the 2′-O-methylation level of *PARP1* mRNA (Fig. 5B, C, *P < 0.05). Furthermore, *FBL* knockdown in the SNORD104-overexpressing HEC1B cells decreased both 2′-O methylated *PARP1* mRNA as well as PARP1 protein levels (Fig. 5D, F, *P < 0.05). The biological role of ribose 2′-O-methylation in mRNA is still unclear, although there are reports that it can improve the stability of nucleic acids against alkaline or enzymatic hydrolysis, most likely by altering their physical and chemical properties [17, 18]. To test this hypothesis, we treated

the SNORD104-overexpressing or knockdown cells with transcription inhibitor actinomycin D. Compared to the control group, the SNORD104-overexpressing cells had significantly higher *PARP1* mRNA stability (Fig. 5G, *P < 0.05), while knocking down either SNORD104 or FBL reduced the stability of *PARP1* mRNA (Fig. 5H, I, *P < 0.05) (Additional file 3).

SNORD104 promotes EC growth by regulating PARP1

PARP1 functions as an oncogene in various cancers [19, 20]. A search of TCGA and CPTAC datasets [10] revealed that *PARP1* RNA and protein levels were significantly increased in EC tissues (Fig. 6A, Additional file 3: Fig. S2A, *P < 0.05). Furthermore, Kaplan–Meier analysis [11] showed the high expression of *PARP1* correlated with poor overall survival (Fig. 6B). To verify whether SNORD104 exerts its carcinogenic effect by regulating *PARP1*, knocked down *FBL* or *PARP1* in the HEC1B cells overexpressing SNORD104 (Fig. 6C, *P < 0.05). As expected, *FBL* or *PARP1*-silencing reversed the effects of SNORD104 on the proliferation (Fig. 6D, E, *P < 0.05), colony formation (Fig. 6F, *P < 0.05), and apoptosis of EC cells (Fig. 6G, *P < 0.05).

Discussion

Endometrial cancer (EC) occurrence and progression involve multiple genetic mutations and epigenetic changes, along with long-term stimulation of estrogen [21, 22]. In recent years, various non-coding RNAs, including long non-coding RNAs, circular RNAs, and small non-coding RNAs, such as microRNAs, piwi-interacting RNAs, and snoRNAs, have been identified that regulate tumor epigenetics. snoRNAs are dysregulated in multiple cancer and are associated with tumor cell growth, metastasis, and self-renewal [23]. For example, SNORD42A promotes acute myeloid leukemia cell proliferation by directing 18S rRNA 2'-O-methylation that promotes protein translation [24]. SNORD89 is highly expressed in ovarian cancer stem cells and promotes dryness of ovarian cancer cells by regulating the Notch1-c-Myc pathway [25]. SNORA74A activates PARP1-directed DExD-box helicase 21 (DDX21) ADP-ribosylation and increases the nuclear localization of DDX21 protein, thereby promoting ribosomal biogenesis and cancer cell growth [26]. However, little is known regarding the role of snoRNAs in EC. To identify the regulatory factors that play a role in the development of EC, we screened for the differentially expressed genes in EC tissues relative to the normal endometrial tissues using the Human Genome Map TCGA Database, and found that SNORD104 and its parent gene *SNHG25* were significantly upregulated in EC tissues. Although the expression levels of a few snoRNAs correlate with that of their host genes [27], the expression and biological functions of most snoRNAs seem to be independent of their host genes [28, 29]. In this study, we found that SNORD104, rather than its host gene *SNHG25*, promotes EC progression. SNORD104 increased the malignant potential of the EC cells in vitro and in vivo, and inhibited apoptosis, thus preliminarily confirming its pro-oncogenic effects in EC (Fig. 7).

The 2′-O-methylation is a relatively conserved type of post-transcriptional modification that is abundant in rRNAs and tRNAs, and protects them against degradation [30]. High-throughput deep sequencing has revealed that 2′-O-ribose methylation exists in the mRNAs and sncRNAs as well [31, 32]. In the present study, RIP experiments showed that SNORD104 binds to *FBL* protein without affecting the latter's expression levels, which further suggests that the biological function of SNORD104 may be exerted via the 2′-O-ribose methylation catalyzed by FBL.

To further confirm this hypothesis, we performed NM-seq in HEC1B cells that overexpressed SNORD104 and identified 928 upregulated 2′-O-methylation sites (671 RNAs). Since snoRNA mainly regulates the modification of target RNAs through complementary base pairing, we intersect the two data sets of Nm-seq and SNORD104-Blast. KEGG pathway enrichment analysis of these RNAs identified that the apoptosis pathway was significantly enriched. Then we analyzed the RNAs enriched in the apoptotic pathway through CPTAC database, and showed that the protein level *of ITPR3, LMNB1, PARP1, PARP4, and TUBA1C* were upregulated in endometrial cancer tissues. Next, RIP assays confirmed that FBL could bind to *PARP1* mRNA, but not the other 4 RNAs, and SNORD104 expression was positively

(See figure on next page.)

Fig. 4 SNORD104 upregulated *PARP1* expression in vitro and in vivo. **A** Immunoprecipitation of SNORD104 using anti-FBL antibodies. **B** Immunoblot showing FBL protein levels in SNORD104-overexpressing HEC1B cells. **C** The 2′-O-methylation level up-regulated RNA in the Nm-seq data set was intersected with the RNA data set of SNORD104-Blast, and the KEGG pathway enrichment analysis showed that the apoptotic pathway ranked first. **D** Anti-FBL antibody was used to perform RIP assay in HEC1B cells, and the mRNA enrichment of PARP1, ITPR3, TUBA1C, PARP4, LMNB1 was detected by qRT-PCR. **E** Evaluation of PARP1, ITPR3, TUBA1C, PARP4, LMNB1 protein levels after overexpression of SNORD104, and only PARP1 RNA and protein level were changed. **F** PARP1 mRNA and protein levels in SNORD104-knockdown Ishikawa cells. **G** SNORD104 and *PARP1* mRNA expression in EC tissues (n = 71) and the correlation between the expression levels (R = 0.3222, P < 0.0001). **H** PARP1 protein levels in the nuclear fraction of SNORD104-overexpressing cells. **I**, **J** PARP1 protein levels in the SNORD104-overexpressing subcutaneous xenografts in nude mice. *P < 0.05, ns means P > 0.05

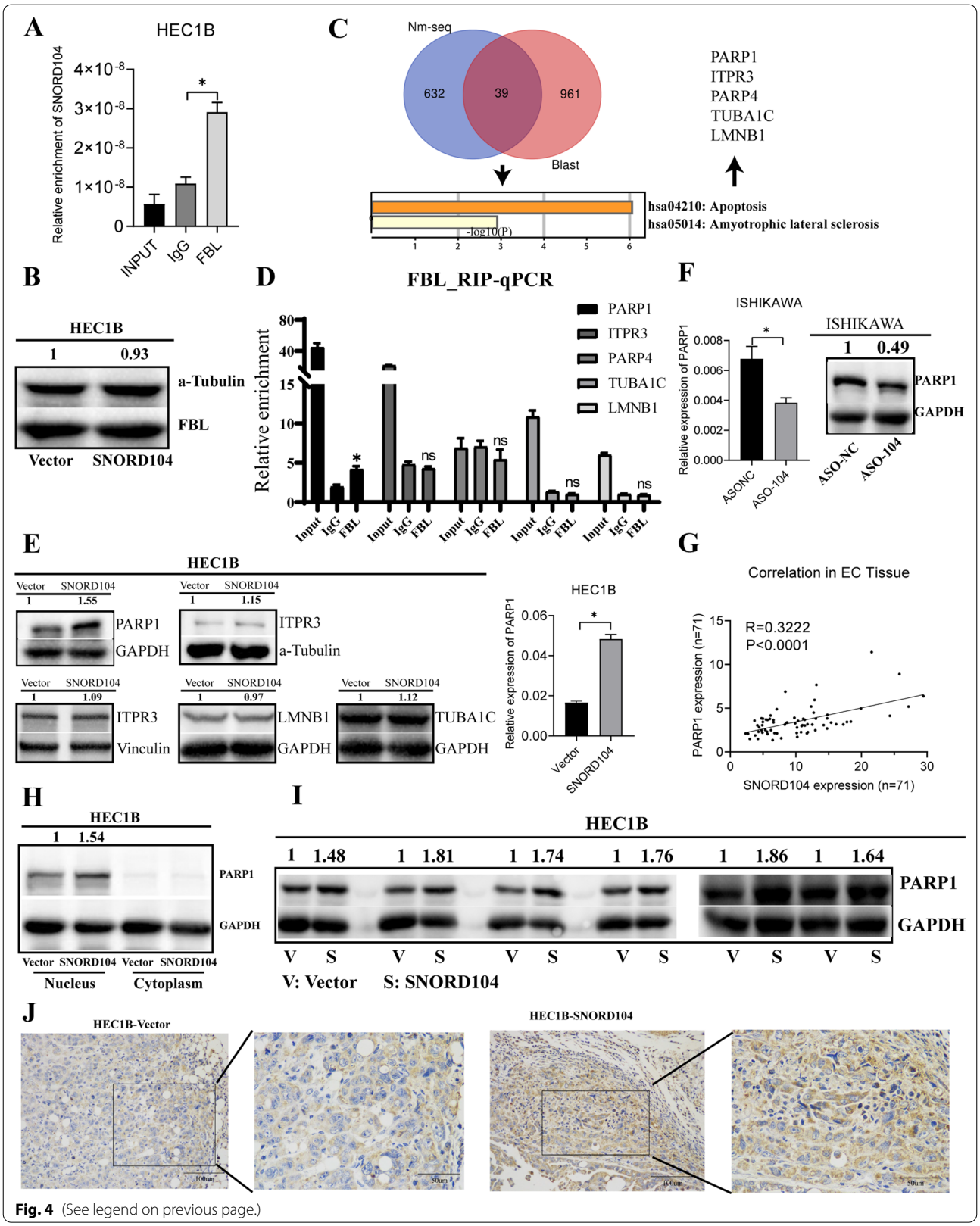

Fig. 4 (See legend on previous page.)

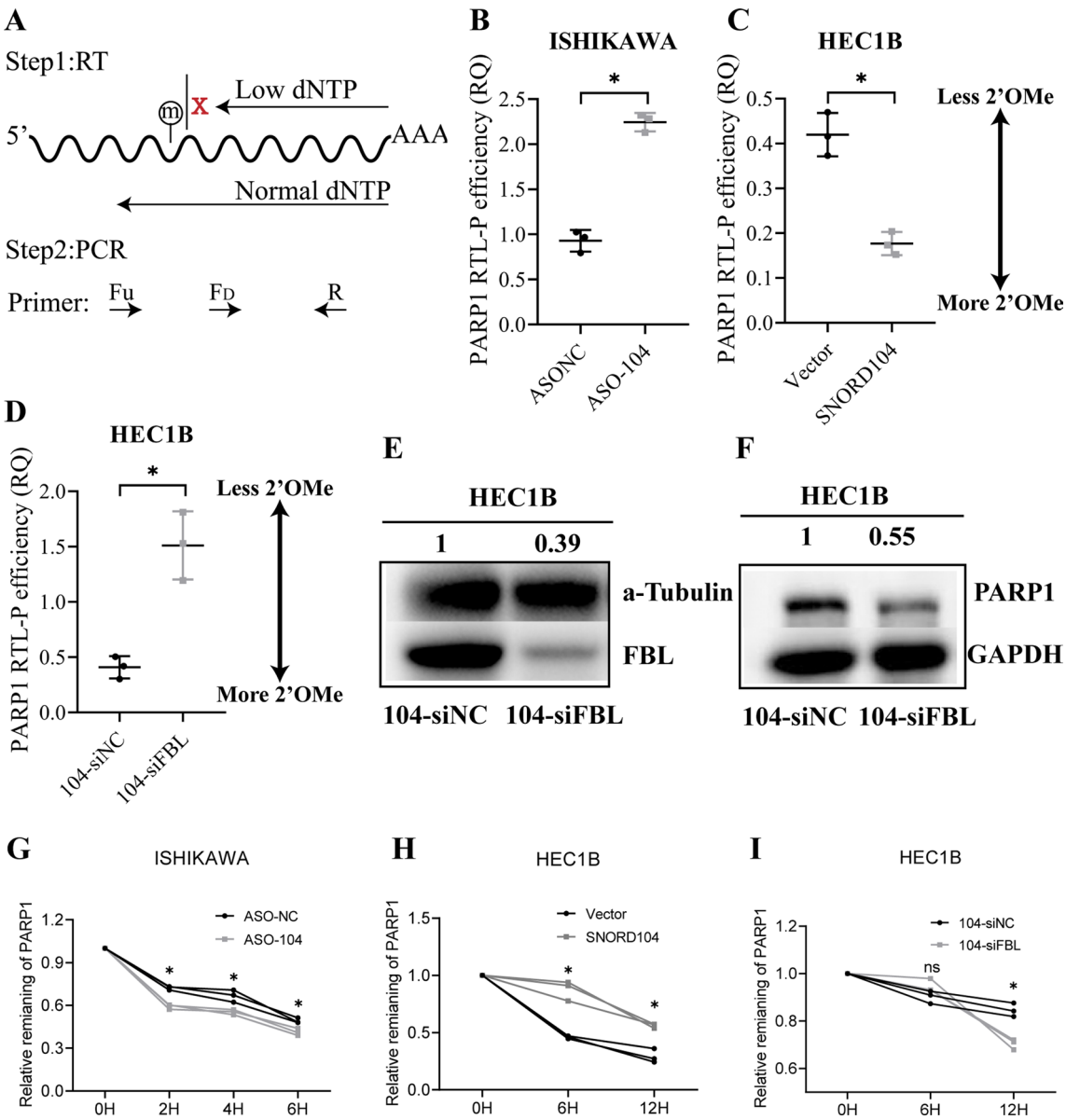

Fig. 5 SNORD104 stabilizes *PARP1* mRNA via 2′-O-methylation. (**A**) Schematic diagram of RTL-P experiment. **B** 2′-O-methylated *PARP1* mRNA levels in SNORD104-knockdown cells. **C** 2′-O-methylated *PARP1* mRNA levels in SNORD104-overexpressing HECB1 cells. **D** 2′-O-methylated *PARP1* mRNA levels in SNORD104-overexpressing HECB1 cells with FBL knockdown. **E**, **F** PARP1 protein levels in SNORD104-overexpressing HECB1 cells with FBL knockdown. **G** *PARP1* mRNA stability in SNORD104-knockdown cells treated with Act D (5 μg/ml). **H** *PARP1* mRNA stability in SNORD104-overexpressing cells. **I** *PARP1* mRNA stability in FBL-knockdown cells. *P < 0.05

correlated with *PARP1* expression in the EC tissues. Previous studies have shown that *PARP1* has two 2′-O-methylation sites at CHR1: 226561928–226561929 and CHR1: 226549725–226549726 [33]. In contrast, our Nm-seq results showed that the modified site was located at CHR1: 226553726–22655372. Subsequently, we verified that SNORD104 regulates 2′-O-methylation of *PARP1* mRNA in EC cells by RTL-P assay. In fact, SNORD104 overexpression or knockdown in EC cells significantly increased or decreased *PARP1* RNA and protein levels.

RNA methylation can regulate target genes [34] by influencing variable splicing [35], increasing RNA stability [36], and regulating RNA transport [37]. To determine the mechanism by which SNORD104-mediated

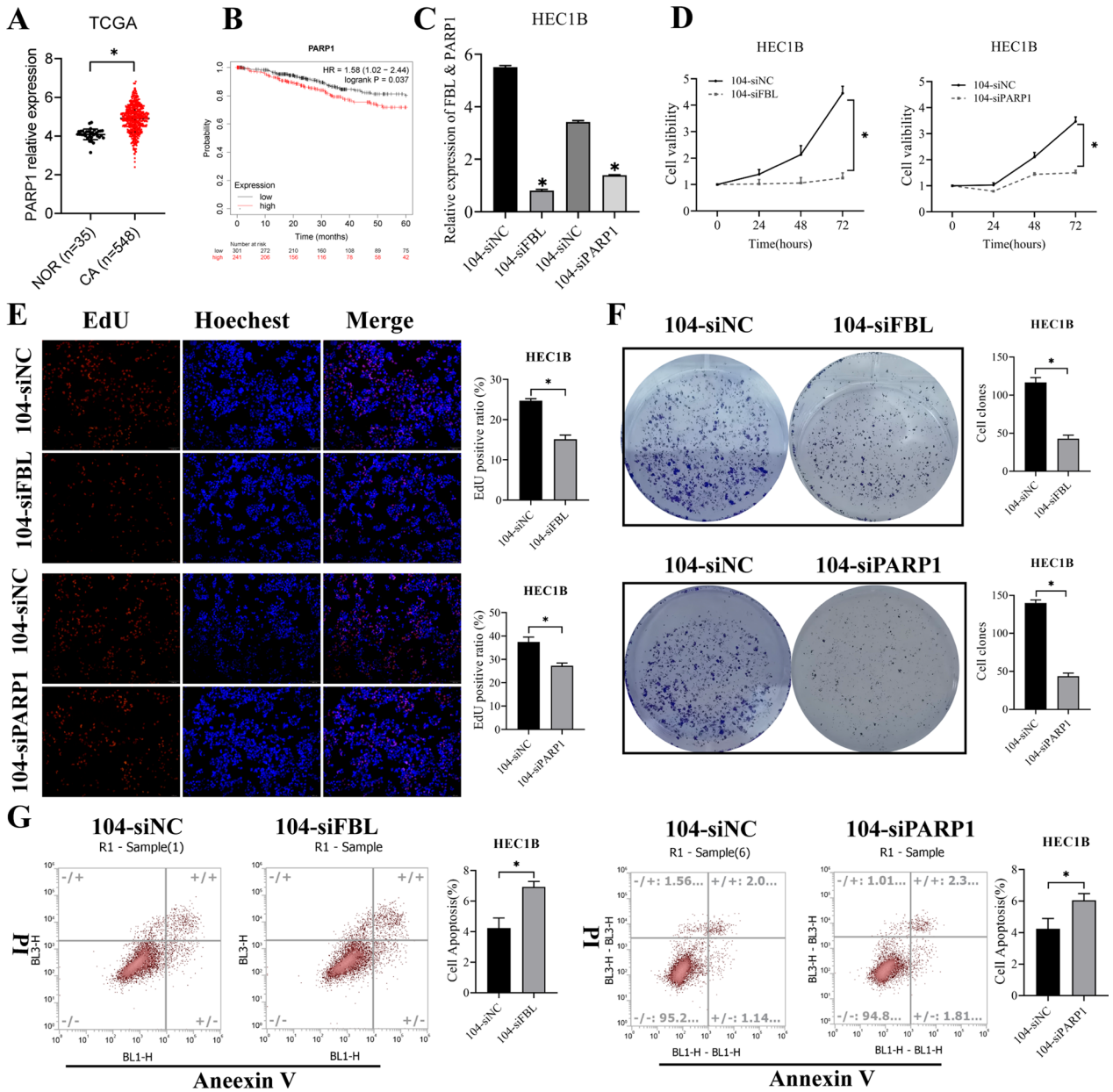

Fig. 6 Knockdown of *FBL* or *PARP1* reversed the carcinogenic effect of SNORD104. **A** *PARP1* RNA levels in the EC tissues in the TGCA dataset. **B** Correlation between *PARP1* expression and 5-year overall survival (OS) of EC patients from the Kaplan–Meier Plotter (P = 0.037). **C** FBL and *PARP1* were knocked down in SNORD104-overexpressing HEC1B cells. The effect of *FBL* or *PARP1* knockdown on the **D**, **E** proliferation, **F** colony formation, and **G** apoptosis of SNORD104-overexpressing cells. *P < 0.05

2′-O-methylation upregulates PARP1 protein, we assessed *PARP1* mRNA stability after treatment with actinomycin D. SNORD104 overexpression or repression significantly enhanced or reduced *PARP1* mRNA stability, respectively. In addition, in HEC1B cells overexpressing SNORD104, *FBL* knockdown reduced the PARP1 protein levels. This suggested that SNORD104 formed a complex with FBL to target and regulate 2′-O-methylation of *PARP1*, thereby increasing its protein level and enhancing its biological function. Finally, to verify that SNORD104 exerts its carcinogenic role by regulating the expression of *PARP1*, we knocked down *FBL* and *PARP1*, respectively, in SNORD104-overexpressing HEC1B cells, which expectedly reversed the oncogenic effects of SNORD104 in EC.

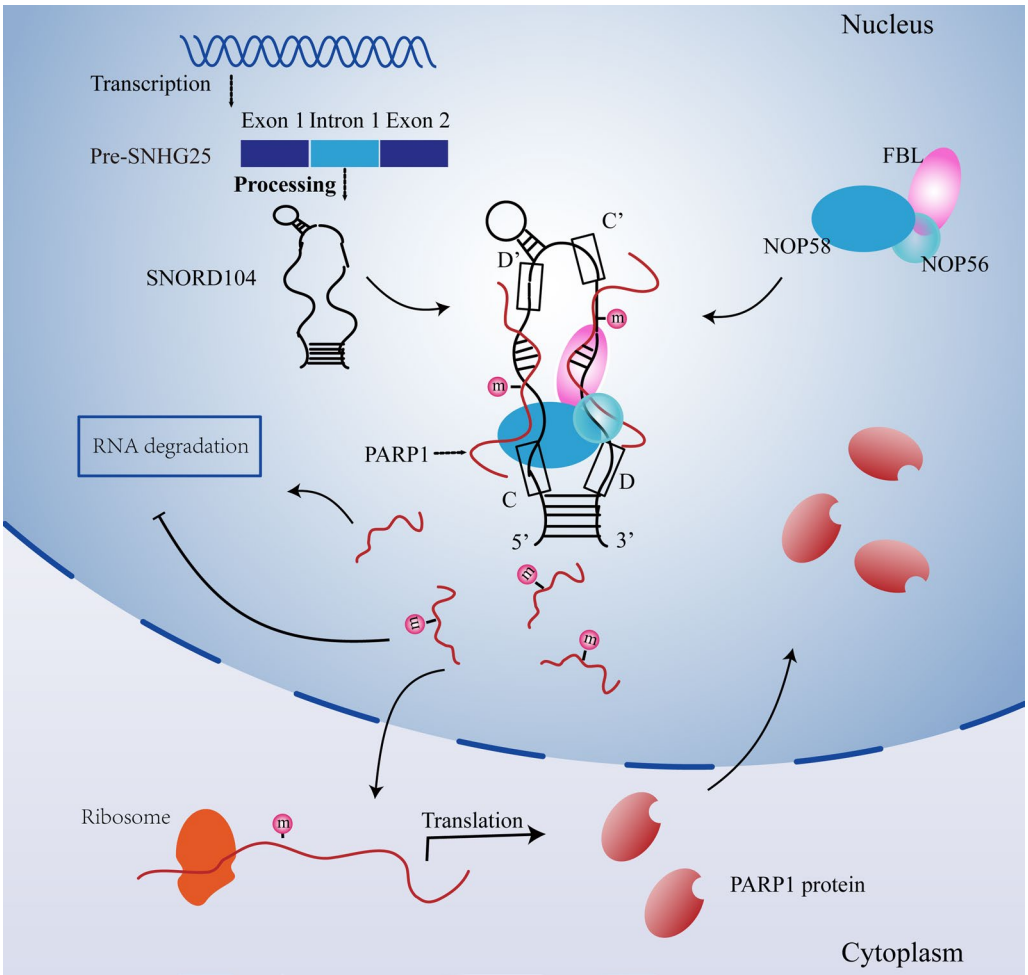

Fig. 7 The mechanism of SNORD104 regulating *PARP1* expression through 2′-O-methylation and promoting EC progression

PARP1, the first member of the *PARP* gene family, is located on chromosome 1 1q42.12, and encodes the chromatin-related enzyme, poly (ADP ribosyl) transferase. PARP1 participates in the poly (ADP-ribosylation) modification induced by DNA damage [38–40]. In addition, PARP1 is an important factor in nucleolar biogenesis. Under non-stress conditions, about 40% of PARP1 molecules are located in the nucleolus [41], where it mediates ribosomal biosynthesis by controlling pre-rRNA processing, post-transcriptional modification, and assembly of pre-ribosomal subunits [42]. Recent studies reported that PARP1 plays a very extensive role in regulating the occurrence and development of tumors, not only participating in cancer cell proliferation, but also participating in metastasis. For instance, it catalyzes poly ADP-ribosylation of *STAT3* (encoding signal transducer and activator of transcription 3) in various cancer cells and subsequently promotes *STAT3* dephosphorylation, resulting in decreased transcription of STAT3 and its target gene *PDL1* (encoding programmed cell death 1 ligand 1) [43]. In breast cancer cells, PARP1 competes with histone H1 to maintain transcription of the oncogene *CCND1* (encoding cyclin D1), and also acts as a transcriptional coactivator of GATA binding protein 3 (GATA3), thus promoting the transcription of *CCND1* [44]. In prostate cancer and kidney cancer, PARP1 is closely related to the metastasis of tumor cells [45, 46]. Thus, PARP1 participates in the occurrence and development of cancer through complex regulatory mechanisms.

Conclusions

SNORD104 is upregulated in EC and promotes tumor growth by inducing 2′-O-methylation of *PARP*1, which enhances the latter's expression and biological function. Our findings provide new insights into the mechanisms underlying the development and progression of EC and

identify novel therapeutic targets for individualized treatment.

Supplementary Information

The online version contains supplementary material available at https://doi.org/10.1186/s12967-022-03802-z.

Additional file 1: Table S1. Correlation of SNORD104 expression with different clinicopathological features of endometrial cancer.

Additional file 2: Fig. S1. Characteristics of *SNHG25* in endometrial cancer. *SNHG25* expression in (A) EC tissues and (B) cell lines. (C&D) *SNHG25* was knocked down in Ishikawa cells and overexpressed in HEC1B cells. (E, F) Effect of *SNHG25* knockdown on the viability and apoptosis of Ishikawa cells. (G, H) Effect of *SNHG25* overexpression on the viability and apoptosis of HEC1B cells. *P < 0.05, ns means P>0.05.

Additional file 3: Fig. S2. SNORD104 potential target RNAs in endometrial cancer. (A) Protein expression of ITPR3, LMNB1, PARP1, PARP4, TUBA1C in endometrial cancer (n=100) and normal endometrial tissue (n=31).

Acknowledgements
Not applicable.

Author contributions
Conceptualization, YZ; formal analysis, XC; investigation, XL, JC and HQ; methodology, BL and SC; project administration, XC, SC and YZ; resources, SC; software, XL and JC; supervision, XC and XL; validation, BL; visualization, HQ; writing—original draft, BL; writing—review and editing, YZ. All authors read and approved the final manuscript.

Funding
This work was supported by the National Natural Science Foundation of China, CHN [No. 82072854; 82272985; 81872115]; Natural Science Foundation of Guangdong Province [No. 2022A1515012293]; the Project for Key Medicine Discipline Construction of Guangzhou Municipality, CHN [No. 2021-2023-17]; Science and Technology Projects in Guangzhou [No. 202201020093; 202201020118]; Young S&T Talent Training Program of Guangdong Provincial Association for S&T(GDSTA) [No. KXRC202214].

Availability of data and materials
The datasets supporting the conclusions of this article are included within the article and its additional file. For any further of the data requests, please contact the corresponding author.

Declarations

Ethics approval and consent to participate
The Ethics Committee of the third affiliated Hospital of Guangzhou Medical University approved the use of human tissue and experimental animals in this study (No: B202108-1). Informed consent was obtained from all patients.

Consent for publication
All authors agree to publication of the article.

Competing interests
The authors declare that no conflict of interests.

Received: 14 September 2022 Accepted: 1 December 2022
Published online: 24 December 2022

References

1. Neri M, Peiretti M, Melis GB, Piras B, Vallerino V, Paoletti AM, et al. Systemic therapy for the treatment of endometrial cancer. Expert Opin Pharmacother. 2019;20:2019–32.
2. Nagle CM, Crosbie EJ, Brand A, Obermair A, Oehler MK, Quinn M, et al. The association between diabetes, comorbidities, body mass index and all-cause and cause-specific mortality among women with endometrial cancer. Gynecol Oncol. 2018;150:99–105.
3. Charo LM, Plaxe SC. Recent advances in endometrial cancer: a review of key clinical trials from 2015 to 2019. F1000Res. 2019;8:849.
4. Romano G, Veneziano D, Acunzo M, Croce CM. Small non-coding RNA and cancer. Carcinogenesis. 2017;38:485–91.
5. Williams GT, Farzaneh F. Are snoRNAs and snoRNA host genes new players in cancer? Nat Rev Cancer. 2012;12:84–8.
6. Liang J, Wen J, Huang Z, Chen XP, Zhang BX, Chu L. Small nucleolar RNAs: insight into their function in cancer. Front Oncol. 2019;9:587.
7. Lui L, Lowe T. Small nucleolar RNAs and RNA-guided post-transcriptional modification. Essays Biochem. 2013;54:53–77.
8. Amin MA, Matsunaga S, Ma N, Takata H, Yokoyama M, Uchiyama S, et al. Fibrillarin, a nucleolar protein, is required for normal nuclear morphology and cellular growth in HeLa cells. Biochem Biophys Res Commun. 2007;360:320–6.
9. Shubina MY, Musinova YR, Sheval EV. nucleolar methyltransferase fibrillarin: evolution of structure and functions. Biochemistry. 2016;81:941–50.
10. Chandrashekar DS, Bashel B, Balasubramanya SAH, Creighton CJ, Ponce-Rodriguez I, Chakravarthi B, et al. UALCAN: a portal for facilitating tumor subgroup gene expression and survival analyses. Neoplasia. 2017;19:649–58.
11. Nagy A, Munkacsy G, Gyorffy B. Pancancer survival analysis of cancer hallmark genes. Sci Rep. 2021;11:6047.
12. Dai Q, Moshitch-Moshkovitz S, Han D, Kol N, Amariglio N, Rechavi G, et al. Nm-seq maps 2′-O-methylation sites in human mRNA with base precision. Nat Methods. 2017;14:695–8.
13. Dong ZW, Shao P, Diao LT, Zhou H, Yu CH, Qu LH. RTL-P: a sensitive approach for detecting sites of 2′-O-methylation in RNA molecules. Nucleic Acids Res. 2012;40:e157.
14. Elliott BA, Ho HT, Ranganathan SV, Vangaveti S, Ilkayeva O, Abou Assi H, et al. Modification of messenger RNA by 2′-O-methylation regulates gene expression in vivo. Nat Commun. 2019;10:3401.
15. Lan T, Yuan K, Yan X, Xu L, Liao H, Hao X, et al. LncRNA SNHG10 facilitates hepatocarcinogenesis and metastasis by modulating Its homolog SCARNA13 via a positive feedback loop. Cancer Res. 2019;79:3220–34.
16. Wu G, Hao C, Qi X, Nie J, Zhou W, Huang J, et al. LncRNA SNHG17 aggravated prostate cancer progression through regulating its homolog SNORA71B via a positive feedback loop. Cell Death Dis. 2020;11:393.
17. Bohnsack MT, Sloan KE. Modifications in small nuclear RNAs and their roles in spliceosome assembly and function. Biol Chem. 2018;399:1265–76.
18. Abou Assi H, Rangadurai AK, Shi H, Liu B, Clay MC, Erharter K, et al. 2′-O-Methylation can increase the abundance and lifetime of alternative RNA conformational states. Nucleic Acids Res. 2020;48:12365–79.
19. Engbrecht M, Mangerich A. The nucleolus and PARP1 in cancer biology. Cancers. 2020;12:1813.
20. Wang L, Liang C, Li F, Guan D, Wu X, Fu X, et al. PARP1 in carcinomas and PARP1 inhibitors as antineoplastic drugs. Int J Mol Sci. 2017;18:2111.
21. Chang Z, Talukdar S, Mullany SA, Winterhoff B. Molecular characterization of endometrial cancer and therapeutic implications. Curr Opin Obstet Gynecol. 2019;31:24–30.
22. Bell DW, Ellenson LH. Molecular genetics of endometrial carcinoma. Annu Rev Pathol. 2019;14:339–67.
23. van der Werf J, Chin CV, Fleming NI. SnoRNA in cancer progression, metastasis and immunotherapy response. Biology. 2021;10:809.
24. Pauli C, Liu Y, Rohde C, Cui C, Fijalkowska D, Gerloff D, et al. Site-specific methylation of 18S ribosomal RNA by SNORD42A is required for acute myeloid leukemia cell proliferation. Blood. 2020;135:2059–70.
25. Zhu W, Niu J, He M, Zhang L, Lv X, Liu F, et al. SNORD89 promotes stemness phenotype of ovarian cancer cells by regulating Notch1-c-Myc pathway. J Transl Med. 2019;17:259.
26. Kim DS, Camacho CV, Nagari A, Malladi VS, Challa S, Kraus WL. Activation of PARP-1 by snoRNAs controls ribosome biogenesis and cell growth via the RNA helicase DDX21. Mol Cell. 2019;75:1270-85.e14.
27. Penzo M, Clima R, Trere D, Montanaro L. Separated siamese twins: intronic small nucleolar RNAs and matched host genes may be altered in conjunction or separately in multiple cancer types. Cells. 2020;9:387.

28. Mei YP, Liao JP, Shen J, Yu L, Liu BL, Liu L, et al. Small nucleolar RNA 42 acts as an oncogene in lung tumorigenesis. Oncogene. 2012;31:2794–804.
29. Fang X, Yang D, Luo H, Wu S, Dong W, Xiao J, et al. SNORD126 promotes HCC and CRC cell growth by activating the PI3K-AKT pathway through FGFR2. J Mol Cell Biol. 2017;9:243–55.
30. Ayadi L, Galvanin A, Pichot F, Marchand V, Motorin Y. RNA ribose methylation (2′-O-methylation): occurrence, biosynthesis and biological functions. Biochim Biophys Acta Gene Regul Mech. 2019;1862:253–69.
31. Nostramo RT, Hopper AK. Beyond rRNA and snRNA: tRNA as a 2′-O-methylation target for nucleolar and Cajal body box C/D RNPs. Genes Dev. 2019;33:739–40.
32. Dimitrova DG, Teysset L, Carre C. RNA 2′-O-methylation (Nm) modification in human diseases. Genes. 2019;10:117.
33. Xuan JJ, Sun WJ, Lin PH, Zhou KR, Liu S, Zheng LL, et al. RMBase v2.0: deciphering the map of RNA modifications from epitranscriptome sequencing data. Nucleic Acids Res. 2018;46:D327–34.
34. Chen XY, Zhang J, Zhu JS. The role of m(6)A RNA methylation in human cancer. Mol Cancer. 2019;18:103.
35. Mendel M, Delaney K, Pandey RR, Chen KM, Wenda JM, Vagbo CB, et al. Splice site m(6)A methylation prevents binding of U2AF35 to inhibit RNA splicing. Cell. 2021;184:3125-42.e25.
36. Marcen R, Dal Canton A. Glomerular filtration rate: utility for assessing long-term renal allograft outcomes in kidney allograft recipients. J Nephrol. 2013;26:1009–24.
37. Roundtree IA, Luo GZ, Zhang Z, Wang X, Zhou T, Cui Y, et al. YTHDC1 mediates nuclear export of N(6)-methyladenosine methylated mRNAs. Elife. 2017;6:e31311.
38. Fischer JM, Popp O, Gebhard D, Veith S, Fischbach A, Beneke S, et al. Poly(ADP-ribose)-mediated interplay of XPA and PARP1 leads to reciprocal regulation of protein function. FEBS J. 2014;281:3625–41.
39. Gibson BA, Kraus WL. New insights into the molecular and cellular functions of poly(ADP-ribose) and PARPs. Nat Rev Mol Cell Biol. 2012;13:411–24.
40. Szabo C, Pacher P, Swanson RA. Novel modulators of poly(ADP-ribose) polymerase. Trends Pharmacol Sci. 2006;27:626–30.
41. Rancourt A, Satoh MS. Delocalization of nucleolar poly(ADP-ribose) polymerase-1 to the nucleoplasm and its novel link to cellular sensitivity to DNA damage. DNA Repair. 2009;8:286–97.
42. Boamah EK, Kotova E, Garabedian M, Jarnik M, Tulin AV. Poly(ADP-Ribose) polymerase 1 (PARP-1) regulates ribosomal biogenesis in *Drosophila nucleoli*. PLoS Genet. 2012;8:e1002442.
43. Ding L, Chen X, Xu X, Qian Y, Liang G, Yao F, et al. PARP1 Suppresses the Transcription of PD-L1 by Poly(ADP-Ribosyl)ating STAT3. Cancer Immunol Res. 2019;7:136–49.
44. Shan L, Li X, Liu L, Ding X, Wang Q, Zheng Y, et al. GATA3 cooperates with PARP1 to regulate CCND1 transcription through modulating histone H1 incorporation. Oncogene. 2014;33:3205–16.
45. Hsu EC, Rice MA, Bermudez A, Marques FJG, Aslan M, Liu S, et al. Trop2 is a driver of metastatic prostate cancer with neuroendocrine phenotype via PARP1. Proc Natl Acad Sci U S A. 2020;117:2032–42.
46. Yang L, Chen Y, Liu N, Shi Q, Han X, Gan W, et al. Low expression of TRAF3IP2-AS1 promotes progression of NONO-TFE3 translocation renal cell carcinoma by stimulating N(6)-methyladenosine of PARP1 mRNA and downregulating PTEN. J Hematol Oncol. 2021;14:46.

Publisher's Note